S-alkylated quinazolin-4(3H)-ones as dual EGFR/VEGFR-2 kinases inhibitors : Design, synthesis, Anticancer Evaluation and Docking Study

Samar S. Tawfik,[a]* Abdelrahman Hamdi,[a]* Ahmed R. Ali,[b] Abdullah A. Elgazar,[c] Hamed W. El-Shafey,[a] Adel S. El-Azab,[d] Ahmed H. Bakheit,[d] Mohamed M. Hefnawy,[d] Hazem A. Ghabbour[e] and Alaa A.-M. Abdel-Aziz[d]

a. Department of Pharmaceutical Organic Chemistry, Faculty of Pharmacy, Mansoura University, Mansoura 35516, Egypt.

b. Department of Medicinal Chemistry, Faculty of Pharmacy, Mansoura University, Mansoura 35516, Egypt.

c. Department of Pharmacognosy, Faculty of Pharmacy, Kafrelsheikh University, Kafr El Sheikh, Egypt

d. Department of Pharmaceutical Chemistry, College of Pharmacy, King Saud University, P. O. Box 2457, Riyadh 11451, Saudi Arabia

e School of Health and Biomedical Sciences, RMIT University, Melbourne 3083, Australia

*Correspondence:
Dr. Samar S. Tawfik, email: drsamarelmasry@mans.edu.eg and Dr. Abdelrahman Hamdi, email: Abdelrahmanhamdi2012@mans.edu.eg

1.1. Molecular Modeling

1.1.1. Molecular Docking Procedure

Crystallographic data of the protein structures were sourced from the RCSB Protein Databank for VEGFR2, which complexed with Sorafenib, and (PDB code 3wze) and EGFR, which was complexed with Lapatinib(PDB code 1XKK). The molecular docking analyses utilized platforms including Discovery Studio, AutoDock 4.2, AutoDock Tools, and PyRx (The Scripps Research Institute, La Jolla, CA). In the initial step, extraneous molecules such as water, ligands, and sulfates were removed from the protein crystal structure using Discovery Studio, preserving only the core protein structure. This refined data was stored as a PDB file. Subsequently, the inclusion of polar hydrogens was achieved with AutoDock Tools, and the resulting structure was stored in the PDBQT format. Using Discovery Studio again, the ligands initially present in the crystal structures were separated and stored as PDB files. The docking tool Pyrx, utilizing both Autodock Vina and Open Babel, was applied in the docking

procedure. The designated grid dimensions for EGFR were 120.485, 18.283, and 21.861 for the x, y, and z axes, respectively, while the grid center was positioned at 16.57 x 32.82 x 38.15 Å, maintaining a spacing of 1.000 Å. In contrast, for VEGFR-2, the grid dimensions were established at 21.635, 17.149, and 22.21 for the x, y, and z axes, respectively, with the grid center at 23.16 x 22.19 x 35.33 Å. The docking simulation was executed through 100 runs, leveraging the Lamarckian Genetic Algorithm. Subsequently, the scoring of free energy (ΔG) was computed. Following the docking simulations, results were visualized using Discovery Studio Visualizer.

1.1.2. Molecular Dynamics (MD) methodology

The binding configurations of compound **4**, showcasing strong affinity towards both EGFR and VEGFR2, underwent MD analysis. These simulations utilized the CHARMM 36 force field [1] and were executed on the NAMD 3 software platform [2]. To prep EGFR and VEGFR2 targets, the CHARMM-GUI online tool [3] was employed, facilitating the creation of topologies for compound **4** via both CHARMM36 and the CHARMM General Force Field (CGenFF) [4]. The main axes of the protein were synchronized with the coordinate axes. Subsequently, these protein-compound systems were immersed in a TIP3P water model within a boxed environment with periodic borders, spanning 15 Angstrom in every direction. To balance the charge, Na^+ and Cl^- ions were introduced at a density of 0.15 mM. For the purpose of energy refinement, a conjugate gradient technique was used, lasting 10,000 iterations. Post-refinement, the systems' temperature was raised to 303.15 K over a span of 500 ps under the NVT condition [5]. Ultimately, they were kept stable at 303.15 K and 1 atm over a 100 ns timeframe through the Langevin piston Nose–Hoover approach. VMD software facilitated the graphical representation and scrutiny of the simulation, encompassing metrics like RMSD, RMSF, Rg, SASA and H-bond evaluations. [6]

References

1. Vanommeslaeghe, K., E. Hatcher, C. Acharya, S. Kundu, S. Zhong, J. Shim, E. Darian, O. Guvench, P. Lopes, and I. Vorobyov, *CHARMM general force field: A force field for drug-like molecules compatible with the CHARMM all-atom additive biological force fields.* Journal of computational chemistry, 2010. **31**(4): p. 671-690.
2. Phillips, J.C., R. Braun, W. Wang, J. Gumbart, E. Tajkhorshid, E. Villa, C. Chipot, R.D. Skeel, L. Kale, and K. Schulten, *Scalable molecular dynamics with NAMD.* Journal of computational chemistry, 2005. **26**(16): p. 1781-1802.
3. Jo, S., T. Kim, V.G. Iyer, and W. Im, *CHARMM-GUI: a web-based graphical user interface for CHARMM.* Journal of computational chemistry, 2008. **29**(11): p. 1859-1865.
4. Vanommeslaeghe, K. and A.D. MacKerell Jr, *Automation of the CHARMM General Force Field (CGenFF) I: bond perception and atom typing.* Journal of Chemical Information and Modeling, 2012. **52**(12): p. 3144-3154.
5. Martyna, G.J., D.J. Tobias, and M.L. Klein, *Constant pressure molecular dynamics algorithms.* The Journal of chemical physics, 1994. **101**(5): p. 4177-4189.
6. Humphrey, W., A. Dalke, and K. Schulten, *VMD: visual molecular dynamics.* Journal of Molecular Graphics, 1996. **14**(1): p. 33-38.
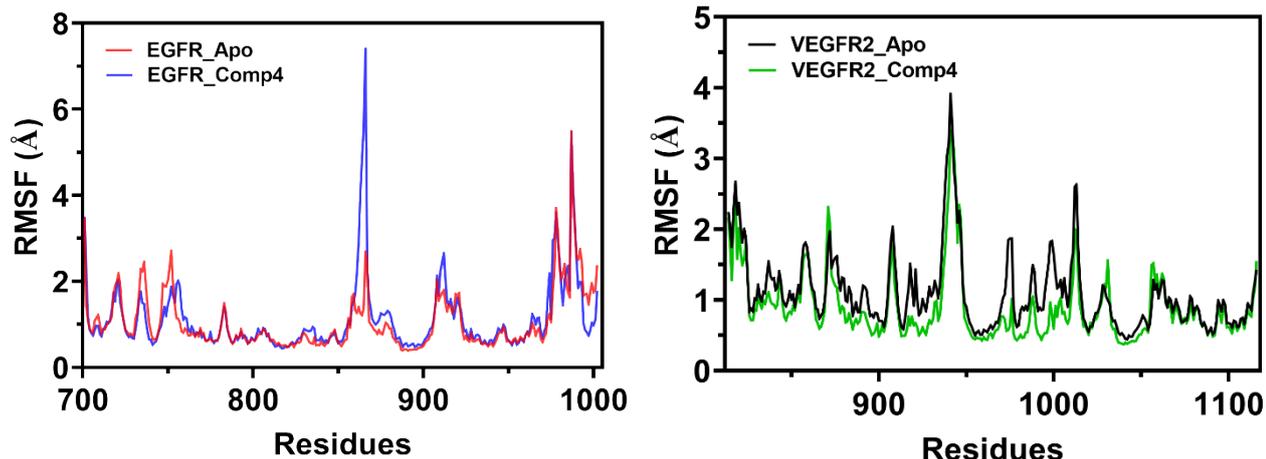
Figure S1. Root Mean Square Fluctuation (RMSF) profiles for EGFR and VEGFR2 in its apo form (depicted in red and black, respectively) and when bound to Comp4 with EGFR and VEGFR2 (illustrated in blue and green, respectively) across different residue positions. The plot showcases the regional flexibility variations of EGFR in both binding states."
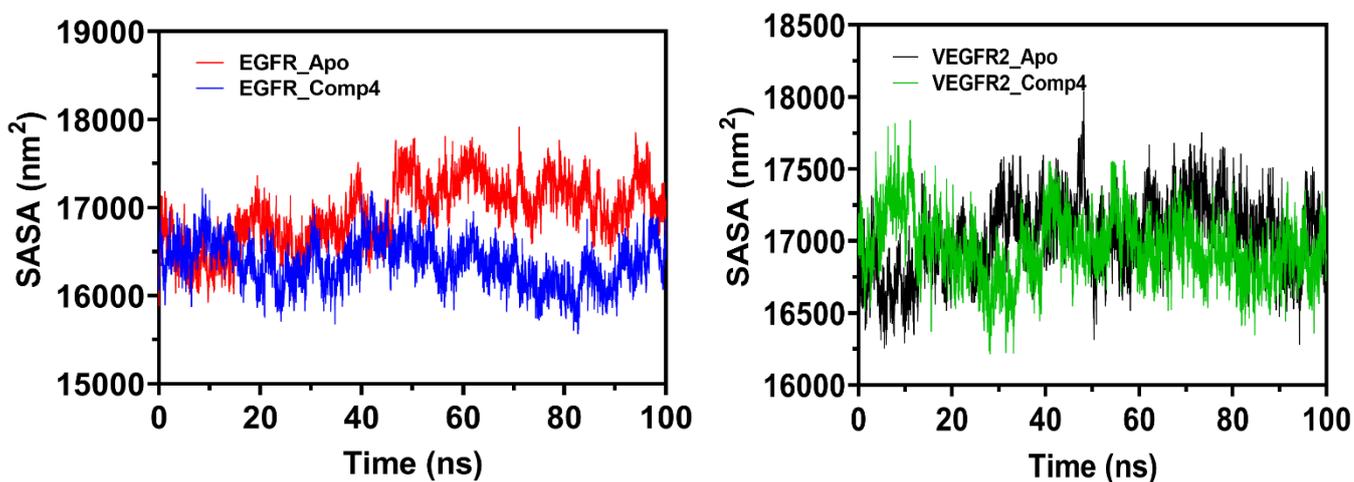

Figure S2. Solvent Accessible Surface Area (SASA) trends of EGFR (red) and VEGFR2 (black) in its and comp4 form (EGFR-comp4) (blue) and (VEGFR2-comp4) (green) .
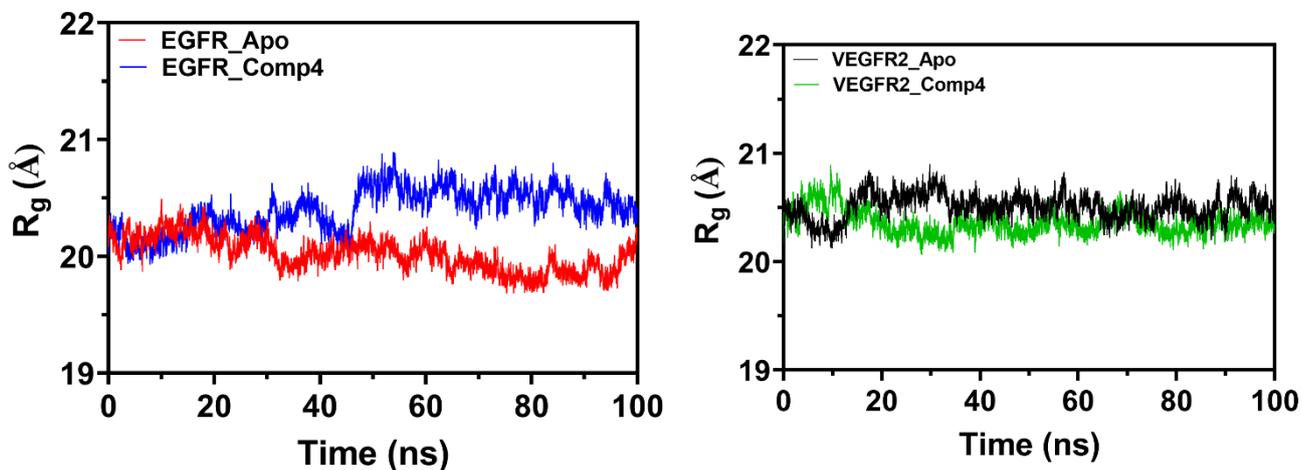
Figure S3. Comparison of the radius of gyration (Rg) between EGFR-Apo (blue curve) and EGFR-comp4 (red curve) over time, highlighting the dynamic structural changes in EGFR-Apo and the relative compactness of EGFR-comp4.
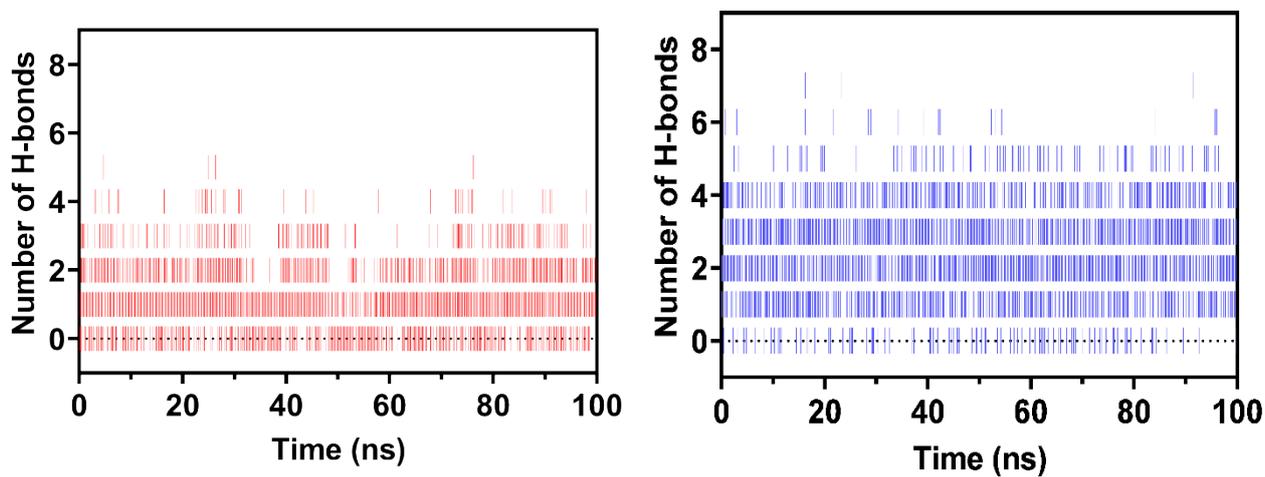

F

igure S4. Hydrogen bonding analysis of Compound 4 with EGFR (red color) for comp4 with VEGFR (blue color).

Table S1. Comparative Analysis of Compounds 4, 11, 20, and Lapatinib Interacting with EGFR (PDB code 1XKK)

Compound	Ligand	Receptor		Interaction	Distance	S (kcal/mol)
Comp 4	H9	A:GLU146:O	Hydrogen Bond	H-Acceptor	2.61	-9.58
	H14	A:TYR211:OH	Hydrogen Bond	H-Acceptor	1.77	
	H16	A:TYR211:OH	Hydrogen Bond	H-Acceptor	2.87	
	H33	A:THR225:OG1	Hydrogen Bond	H-Acceptor	2.86	
	6-ring	A:CYS290:SG	Other	π-Sulfur	5.64	
	S3	A:TYR211	Other	π-Sulfur	3.61	
Comp 5g	H17	A:TYR211:OH	Hydrogen Bond	H-donor	1.66	-8.80
	Cl42	A:PRO214:CD	Hydrogen Bond	H-acceptor	3.08	
	6-ring	A:ARG187:NH1	Electrostatic	H-acceptor	3.31	
	C 19	A:GLU147:OE2	Electrostatic	Pi-Donor	4.03	
	N 15	A:TYR211:OH	Hydrogen Bond	H-donor	3.51	
	6-ring	A:MET1002:SD	Other	Pi-Sulfur	5.285	
Comp 20	H 20	A:ASP855:OD2		H-donor	2.364	-8.67
	6-ring	A:LEU844:CD2		Pi-Sigma	3.837	
LPB	H 6	A:MET793:O		H-Acceptor	2.937	-10.69
	H 39	A:ASP800:OD2		H-Acceptor	1.673	
	F 29	A:CYS775:O		Halogen Acceptor	3.213	
	F 29	A:ARG776:C		Halogen Acceptor	3.387	
	6-ring	A:ASP855:N		pi-H	4.156	

Table S2. Summary of Key Molecular Interactions between Investigational Compounds and VEGFR-2 Kinase Domain (PDB: 3WZE)

Compound	Ligand	Receptor	Interaction	Distance	S (kcal/mol)
Comp 4	HN	A:ASP1046:HN	H-donor	1.982	-9.49
	H17	A:GLU885:OE2	H-Acceptor	2.085	
	S13	A:GLU885:OE2	Sulfur-X	3.134	
	6-ring	A:ASP1046:OD2	Pi-Anion	3.719	
Comp 11	H 17	A:GLU885:OE2	H-acceptor	2.915	-8.31
	H 17	A:ASP1046:O	H-acceptor	2.705	
	6-ring	A:ASP1046:OD2	Pi-Anion	2.908	
Comp 20	O23	A:LYS868:HZ1	H-Donor	2.907	-9.43
	O18	A:ASP1046:HN	H-Donor	2.199	
	H17	A:GLU885:OE2	H-Acceptor	1.810	
	O11	A:HIS1026:CA	H-Donor	3.364	
	6-ring	A:ASP1046:OD2	Pi-Anion	4.295	
SFB	F23	A:HIS1026:HE2	H-Donor	2.446	-12.01
	O10	A:ASP1046:H	H-Donor	2.203	
	H11	A:GLU885:OE2	H-Acceptor	1.935	
	H12	A:GLU885:OE2	H-Acceptor	2.09	
	H34	A:CYS919:O	H-Acceptor	2.04	
	C27	A:GLU917:O	H-Acceptor	3.235	
	C35	A:LYS920:O	H-Acceptor	3.689	
	F21	A:ILE1044:O	Halogen Acceptor	2.611	